



HAL
open science

Responsivity Measurements up to 110 GHz Using AlGaN/GaN HEMTs with Different Gate Size

Ignacio Íñiguez-De-La-Torre, Philippe Artillan, Gaudencio Paz-Martínez, Edouard Rochefeuille, Tomás González, Javier Mateos

► **To cite this version:**

Ignacio Íñiguez-De-La-Torre, Philippe Artillan, Gaudencio Paz-Martínez, Edouard Rochefeuille, Tomás González, et al.. Responsivity Measurements up to 110 GHz Using AlGaN/GaN HEMTs with Different Gate Size. 2023 International Workshop on Integrated Nonlinear Microwave and Millimetre-Wave Circuits (INMMIC), IEEE, pp.1-3, 2023, 10.1109/INMMIC57329.2023.10321787 . hal-04712808

HAL Id: hal-04712808

<https://hal.science/hal-04712808v1>

Submitted on 27 Sep 2024

HAL is a multi-disciplinary open access archive for the deposit and dissemination of scientific research documents, whether they are published or not. The documents may come from teaching and research institutions in France or abroad, or from public or private research centers.

L'archive ouverte pluridisciplinaire **HAL**, est destinée au dépôt et à la diffusion de documents scientifiques de niveau recherche, publiés ou non, émanant des établissements d'enseignement et de recherche français ou étrangers, des laboratoires publics ou privés.

Responsivity Measurements up to 110 GHz Using AlGaN/GaN HEMTs with Different Gate Size

I. Íñiguez-de-la-Torre,¹ Philippe Artillan,² Gaudencio Paz-Martínez¹, Edouard Rochefeuille,² T. González,¹ and J. Mateos¹
¹Applied Physics Department and NANOLAB USAL Universidad de Salamanca, Salamanca, Spain
²CNRS, Grenoble INP, IMEP-LAHC, Univ. Grenoble Alpes, Grenoble, France
indy@usal.es

Abstract—The responsivity of microwave zero-bias detectors based on GaN high electron mobility transistors (HEMTs) is measured up to 110 GHz. A compact model based on static coefficients extracted from the DC output curves together with S-parameter measurements is able to replicate the detection results both when the radio-frequency power is fed into the drain or the gate terminals. A detailed analysis of the contribution of the gate-drain coupling to the RF responsivity allows to identify the origin of the frequency roll-off when shrinking the gate-size of the transistors.

Index Terms—Device physics, GaN high electron mobility transistors (HEMTs), Radio frequency detection, Zero-bias detector

I. INTRODUCTION

In recent years, Field Effect Transistors (FETs) have started to be used as sensitive RF detectors up to frequencies above their cutoff for its classic amplification function. In Refs. [1], [2], a complete review of the state-of-the-art FET-based THz detectors is presented. At sub-THz frequencies, FET-based RF detectors operate through a resistive mixing mechanism, in which the RF signal injected into the gate or drain terminals provides a non-zero DC current (or voltage) due to the device non-linearity. An external gate-drain capacitance is commonly added to the transistor in the case of gate injection to enhance the coupling of the signal to the drain port and allow for RF detection at low frequencies. In this work we analyze standard high electron mobility transistors (HEMTs) fabricated on an AlGaN/GaN heterojunction without external elements, which are more suitable for understanding the physics behind the detection process. We study their performance in zero-bias current detection mode (with short-circuited drain) with different gate geometries. In the literature several authors have tried to compute the frequency-dependent detection of FETs [3], [4], making use of strong assumptions. Here we will use a recently proposed analytical model based on static coefficients obtained from DC measurements, which, together with the S-matrix obtained from the RF characterization of the devices, is able to explain the mechanisms behind the observed dependencies of the detection experiments [5].

This work has been partially supported through Grant PID2020-115842RB-I00 funded by MCIN/AEI/10.13039/501100011033.

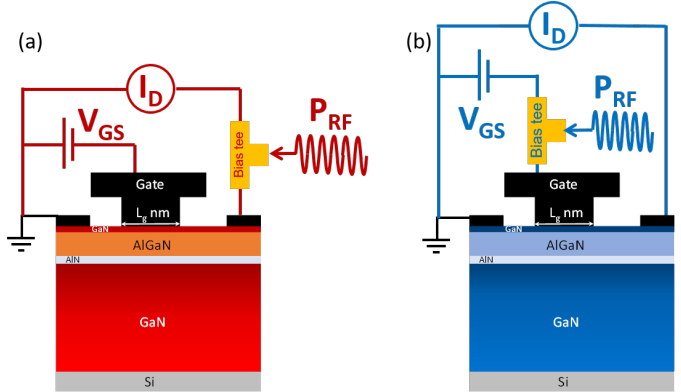


Fig. 1. Schematic drawing of the two configurations used for current detection: (a) RF power injected into the drain (DI) and (b) into the gate (GI). An internal bias-tee allows to couple DC and RF signals. One channel of the SMU is used both to bias the drain with $V_{DS}=0$ V and measure the drain current I_D , and the other to apply the gate voltage V_{GS} .

II. DEVICE UNDER TEST AND EXPERIMENTAL SETUP

Our devices under test are HEMTs with an AlGaN/GaN heterojunction grown on a high-resistivity Si substrate [6]. The heterostructure has a 14 nm thick AlGaN (29% Al) layer, on a 1.73 μm thick GaN buffer, with an 1 nm spacer of AlN in the middle to improve carrier confinement in the 2DEG, and a GaN cap of 0.5 nm thick on the top of the heterostructure. Additionally, they have been passivated with a N_2O pretreatment and 150 nm of SiN. Hall measurements of the wafer have provided a mobility of about 2000 cm^2/Vs . These transistors exhibit cutoff frequencies above 100 GHz.

In this contribution, measurements of current responsivity have been performed in two transistors with $L_G=75$ nm ($W=2 \times 25$ μm , called T-75) and $L_G=250$ nm ($W=2 \times 50$ μm , called T-250), both with $L_{DS}=2.5$ μm . The experiments of RF detection were performed using the same setup described in [7], with the RF source being a VNA with a frequency range from 10 MHz to 67 GHz. In this contribution, frequency extenders have been added to increase the test frequency up to 110 GHz. The insertion losses of the cables and RF probes have been taken into account to actually deliver a constant RF power, P_{RF} , at the reference plane of the transistor. Moreover, a power-meter has been used to calibrate the power in 75-

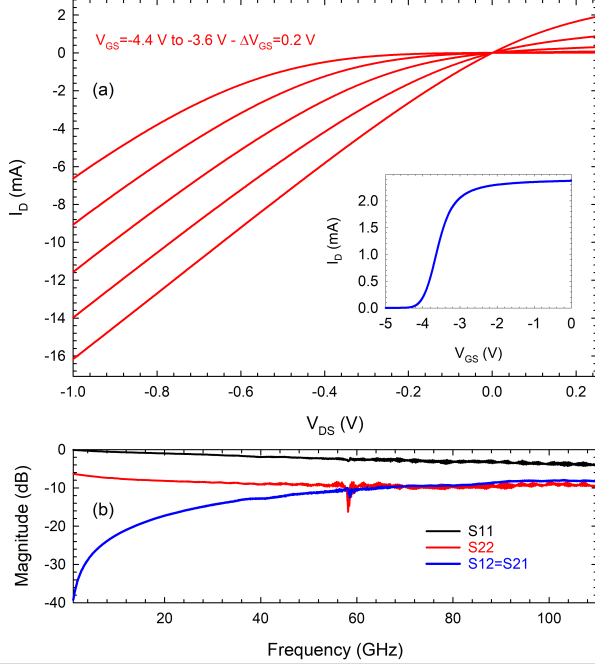


Fig. 2. (a) Output I_D - V_{DS} curves and (b) S-parameters for $V_{DS}=0$ V and $V_{GS}=-3.8$ V of the transistor T-75. The inset shows the transfer curve measured at $V_{DS}=0.1$ V.

110 GHz band. The RF signal can be injected into the drain (DI) or the gate (GI) ports of the HEMTs, see Fig.1, while the detected DC current response in both schemes is measured and averaged at the (short-circuited) drain terminal. Here we focus intentionally in zero-voltage bias detection, $V_{DS}=0$ V, in order to minimize the output noise and improve the sensitivity. The responsivity is obtained as the ratio $\beta = \frac{\Delta I_D}{P_{RF}}$, where ΔI_D is the DC shift of I_D caused by the RF excitation and a subscript d or g is added to distinguish between DI and GI schemes (β_d and β_g).

III. RESULTS AND DISCUSSION

A. DC Curves and S-parameters

The ingredients for our model will be (i) the non-linearity of the transistor, accounted for by the measured DC curves, and (ii) its frequency dependent behavior, described by the S-parameter data, both shown in Fig. 2 for the T-75 HEMT. In (b), the bias point for maximum detection $V_{GS}=-3.8$ V has been chosen for the presentation of the S-parameters and, as usual, the drain is connected to port 2 of the VNA while the gate correspond to port 1.

B. Current Responsivity for Different Gate Size

Fig. 3 shows the typical bell shape dependence of β_d on V_{GS} , showing a maximum (in absolute value, since it takes negative values) for a gate bias slightly above the threshold voltage. At low frequency, 1 and 20 GHz, β_d is almost frequency independent, but decreases at high frequency, being

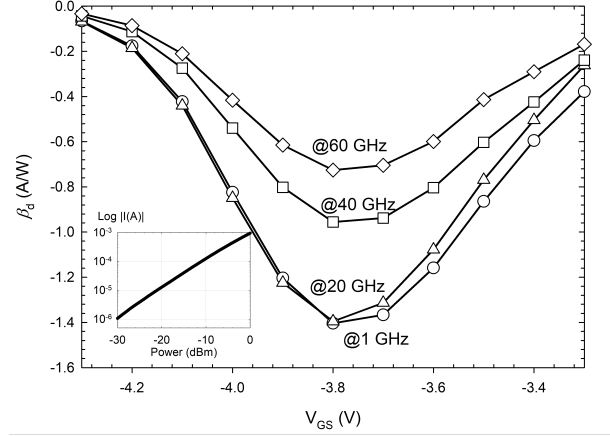


Fig. 3. Current responsivity β_d in A/W as a function of V_{GS} measured in the transistor T-75 for different values of the frequency of the injected RF signal (with -20 dBm power). The inset shows the output current vs. input RF power (at 1 GHz frequency), showing a quasi-ideal square law response.

almost halved at 60 GHz. Moreover, the inset shows a practically ideal square law response of the T-75 HEMT at 1 GHz, with a large dynamic range of more than 30 dB. The frequency dependence of both β_d and β_g (and for both T-75 and T-250), is plotted in Fig. 4 for the V_{GS} value where the maximum responsivity takes place for each transistor. The maximum value of β_d follows the expected behaviour: it is proportional to W and almost independent of L_G , while its frequency roll-off, typically characterized by the -3 dB frequency (f_{3dB} , corresponding to a halved responsivity), appears at higher frequencies with the reduction of both L_G and W due to the smaller gate capacitance (mainly C_{gd}). Indeed, f_{3dB} increases from about 20 GHz for T-250 to about 30 GHz for the HEMT with half W ($L_G=250$ nm $W=2 \times 50$ μ m, not shown here), and to 60 GHz for T-75. This happens because the drain-gate coupling, which has a positive contribution to the current detection (opposite to the negative one associated to the direct drain rectification [3], the only one appearing at low frequency in β_d) is practically proportional to C_{gd} . It is this fact which makes more complex the frequency behaviour of the responsivity for the GI configuration, β_g . It is null at low frequency, as the drain-gate coupling is needed for having a non-zero value of I_D for $V_{DS}=0$ V. In absence of an external C_{gd} capacitor, the increase of β_g coincides with the frequency roll-off of the transistor detection, so that no plateau is observed in the β_g vs. f behaviour, Fig. 4(b).

In [3] we have proposed a generic high frequency model of two-port RF detectors were a closed-form expression, based on (i) the static coefficients defined as $g_{ij} = \partial^{(i+j)} I_D / \partial^i V_{GS} \partial^j V_{DS}$ extracted from the I_D - V_{DS} curves and (ii) measured the S-parameters, is able to replicate both responsivities using the following equations:

$$\beta_d = \frac{R_0}{2} \left(g_{20} |S_{12}|^2 + g_{02} |1+S_{22}|^2 + 2g_{11} \Re[S_{12}^*(1+S_{22})] \right), \quad (1)$$

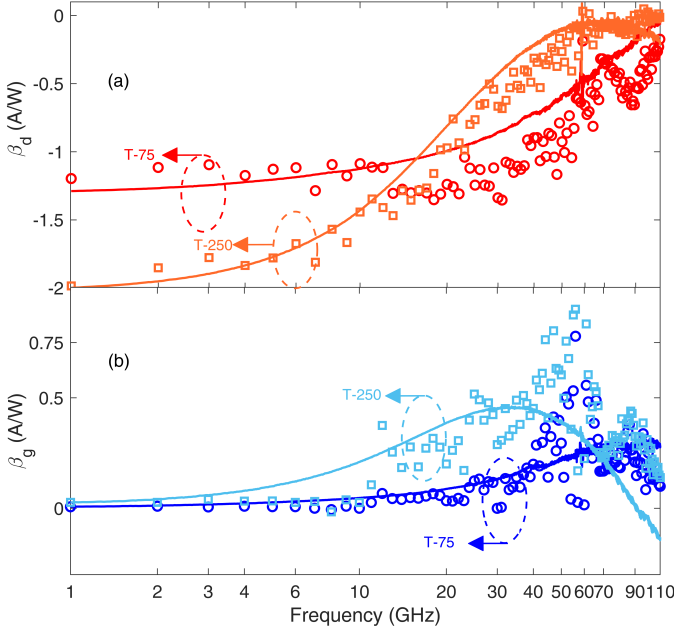


Fig. 4. Measurements (symbols) of (a) β_d and (b) β_g compared to the results of the proposed model (lines) given by eqs. (1) and (2), respectively, as a function of the excitation frequency for the two HEMTs T-75 and T-250.

$$\beta_g = \frac{R_0}{2} \left(g_{20} |1+S_{11}|^2 + g_{02} |S_{21}|^2 + 2g_{11} \Re[S_{21}^*(1+S_{11})] \right), \quad (2)$$

where $R_0=50\Omega$ is the typical output impedance of the source. The results of the model, presented by lines in Fig. 4, which accurately reproduce the DI and GI detection experiments in all the frequency span, will be used to explain the observed dependencies on the gate length and width.

C. Contributions to the Responsivity

The contributions of each term of eqs. (1) and (2) are plotted in Fig. 5, the one proportional to g_{02} representing the direct drain detection, and that on g_{11} associated to the gate-drain coupling. Note that for a zero-bias detector the term proportional to g_{20} is null (a non-null drain voltage is needed for having a current output). It is now clear that the frequency roll-off of the RF detection within the DI configuration is mainly due to the contribution of the of the gate-drain coupling (opposite to the direct drain detection), which appears at higher frequencies as C_{gd} is reduced. Conversely, the increase of β_g , also linked to that same mechanism, follows similar trends.

IV. CONCLUSIONS

We demonstrate zero-bias microwave power detection up to 110 GHz with GaN HEMTs in two schemes, DI and GI. A robust model is able to replicate the frequency dependence of the experiments and explain its physical origin. The decrease in the DI responsivity coincides with the increase of the GI one, due to the capacitive gate-drain coupling. We demonstrate that the high frequency roll-off of the detection can be optimized with the reduction of both L_G and W due to the smaller gate-drain capacitance.

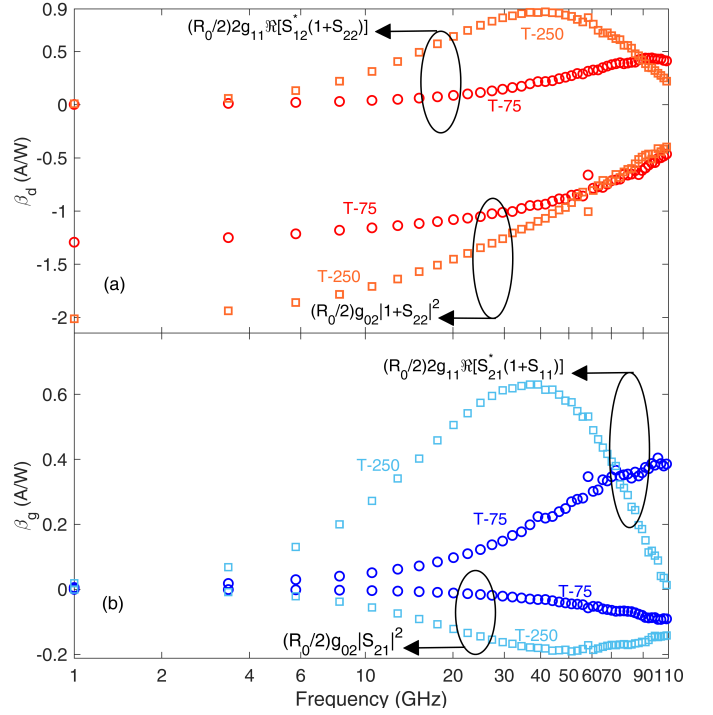


Fig. 5. Contribution of each term of (a) eq. (1) to β_d and (b) eq. (2) to β_g .

REFERENCES

- [1] F. Aniel, G. Auton, D. Cumming, M. Feiginov, S. Gebert, T. González, C. Li, A. Lisauskas, H. Marinchio, J. Mateos, C. Palermo, A. Song, J. Treuttel, L. Varani and N. Zerounian, "Springer Handbook of Semiconductor Devices", 2023.
- [2] E. Javadi, D. B. But, K. Ikamas, J. Zdanevičius, W. Knap and A. Lisauskas, "Sensitivity of field-effect transistor-based terahertz detectors", *Sensors*, vol. 21, no. 9, pp. 2909, 2021
- [3] M. A. Andersson and J. Stake, "An Accurate Empirical Model Based on Volterra Series for FET Power Detectors", *IEEE Trans. Microw. Theory Techn.*, vol. 64, no. 5, pp. 1431-1441, 2016.
- [4] M. I. W. Khan, S. Kim, D.-W. Park, H.-J. Kim, S.-K. Han, and S.-G. Lee, "Nonlinear analysis of nonresonant THz response of MOSFET and implementation of a high-responsivity cross-coupled THz detector", *IEEE Trans. Terahertz Sci. Technol.*, vol. 8, no. 1, pp. 108-120, 2018
- [5] G. Paz-Martínez, P. Artillan, J. Mateos, E. Rochefeuille, T. González and I. Íñiguez-de-la-Torre, "A Closed-Form Expression for the Frequency Dependent Microwave Responsivity of Transistors Based on the I-V Curve and S-Parameters," *IEEE Trans. Microw. Theory Techn.*, DOI: 10.1109/TMTT.2023.3291391
- [6] P. Altuntas et. al, "Power performance at 40 GHz of AlGaIn/GaN high-electron mobility transistors grown by molecular beam epitaxy on Si(111) substrate", *IEEE Elec. Dev. Lett.*, vol. 36, no. 4, pp. 303-305, 2015.
- [7] G. Paz-Martínez, I. Íñiguez-de-la-Torre, H. Sánchez-Martín, T. González and J. Mateos, "Analysis of GaN-based HEMTs operating as RF detectors over a wide temperature range", *IEEE Trans. Microw. Theory Techn.*, DOI: 10.1109/TMTT.2023.3238794.